

# Turbulence stabilization

Yu Mao<sup>1</sup> and Jérôme Gilles<sup>2</sup>

<sup>1</sup> Institute for Mathematics and Its Applications, University of Minnesota, 425 Lind Hall 207 Church Street SE, Minneapolis, MN 55455-0134, USA

<sup>2</sup> Department of Mathematics, University of California Los Angeles, 520 Portola Plaza, Los Angeles, CA 90095-1555, USA

## ABSTRACT

We recently developed a new approach to get a stabilized image from a sequence of frames acquired through atmospheric turbulence. The goal of this algorithm is to remove the geometric distortions due by the atmosphere movements. This method is based on a variational formulation and is efficiently solved by the use of Bregman iterations and the operator splitting method. In this paper we propose to study the influence of the choice of the regularizing term in the model. Then we proposed to experiment some of the most used regularization constraints available in the litterature.

**Keywords:** Stabilization, Turbulence restoration, Regularization constraints, Bregman Iterations

## 1. INTRODUCTION

These last few years show an increase of interest in the development of mitigation algorithms to deal with the atmospheric turbulence degradations. Indeed, turbulences can affect images in two major ways: a blurring effect and random geometric distortions.

An interesting work about turbulence modelization for mitigation algorithms was made by Frakes.<sup>15,16</sup> The authors modeled the turbulence phenomenon by using two operators:

$$f_i(x) = D_i(H(u(x))) + \text{noise} \quad (1)$$

where  $u$  is the static original scene we want to retrieve,  $f_i$  is the observed image at time  $i$ ,  $H$  is a blurring kernel, and  $D_i$  is an operator which represents the geometric distortions caused by the turbulence at time  $i$ . Based on this model, the idea is to try to inverse the two operators  $H$  and  $D_i$ . Inversing  $H$  is a deconvolution problem which will not be addressed here (we propose an original deconvolution approach in<sup>20</sup>), in this paper we will focus on the stabilization problem to remove the geometric distortions.

In a recent work,<sup>29</sup> we proposed a new variational framework based on a combination of a deformation flow estimation and a nonlocal regularization term to retrieve a stabilized image from a set of acquired frames. Our results clearly outperform other existing methods like the PCA-based algorithm<sup>26</sup> or the Lucky-Region Fusion approach.<sup>2</sup> If our algorithm is very efficient and needs very few images (20 input frames seem enough in all the cases), its main drawback is the computational time needed to apply the nonlocal regularization. In this paper, we propose to study the impact, in terms of image quality reconstruction, the choice of other regularizers.

The reminder of the paper is as follows. In section 2 we recall the model developped in.<sup>29</sup> Section 3 presents the different regularizer we choose to test instead of the nonlocal one. Corresponding experiments are presented in section 4 and some conclusions are provided in section 5.

---

Further author information: (Send correspondence to Jérôme Gilles)

Yu Mao: maoya004@ima.umn.edu

Jérôme Gilles: jegilles@math.ucla.edu, Telephone: 1 310 794 7737, <http://www.math.ucla.edu/~jegilles>

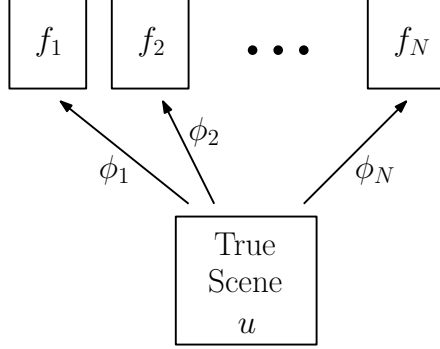


Figure 1. The model of deformation used in the restoration process.

## 2. THE STABILIZATION MODEL

In,<sup>29</sup> we proposed to use the following variational model (2) to find a restored image from a set of input frames.

$$\min_{u, \phi_i} J(u) \quad \text{s.t.} \quad f_i = \Phi_i u + \text{noise}, \quad \forall i \quad (2)$$

Where the observed image sequence is denoted  $\{f_i\}_{i=1, \dots, N}$  and  $u$  the true image that needs to be reconstructed. Each  $\phi_i$  corresponds to the geometric deformation on the  $i$ -th frame (note that the  $\phi_i$  are the deformations between the true image and the observed frame  $i$  and not the continuous movement flow from frame to frame, see Fig. 1). The term  $J(u)$  is the regularizer applied to the reconstructed image, we will discuss its choice in the next section.

Such models can be efficiently solved by the alternative optimization method, i.e. optimizing over the different  $u, \phi_i$  variables alternatively.

In our model (2), if we have a good guess on  $u$ , then the optimal  $\phi_i$  can be estimated via certain optical flow algorithms (e.g. the methods developed in<sup>3,4,33</sup>). On the other hand, for fixed  $\{\phi_i\}$  and by setting  $\sum_i \|\Phi_i u - f_i\|_2^2$  be the data fidelity term, the model (2) can be rewritten as a constrained problem and efficiently solved via Bregman Iterations<sup>30</sup> (see<sup>29</sup> for more details about the model).

The overall Algorithm 1 is as follows:

---

**Algorithm 1** The Alternative Optimization Algorithm

---

Initialize: Start from some initial guess  $u$ . Let  $\tilde{f}_i = f_i$ .

**while**  $\sum_i \|\Phi_i u - f_i\|^2$  not small enough **do**

    Estimate  $\Phi_i$  which maps  $u$  onto  $f_i$  via optical flow.

**while**  $\sum_i \|\Phi_i u - \tilde{f}_i\|^2$  not converge **do**

$$v \leftarrow u - \delta \sum_i \Phi_i^\top (\Phi_i u - \tilde{f}_i)$$

$$u \leftarrow \arg \min_u J(u) + \frac{\lambda}{2\delta} \|u - v\|^2$$

**end while**

$$\tilde{f}_i \leftarrow \tilde{f}_i + f_i - \Phi_i u.$$

**end while**

---

The initial value of  $u$  is chosen as the temporal average of the frames; it is very blurry but gives a good initial guess of the rough shape of the object. The quantity of frames determines the reconstruction quality. On the

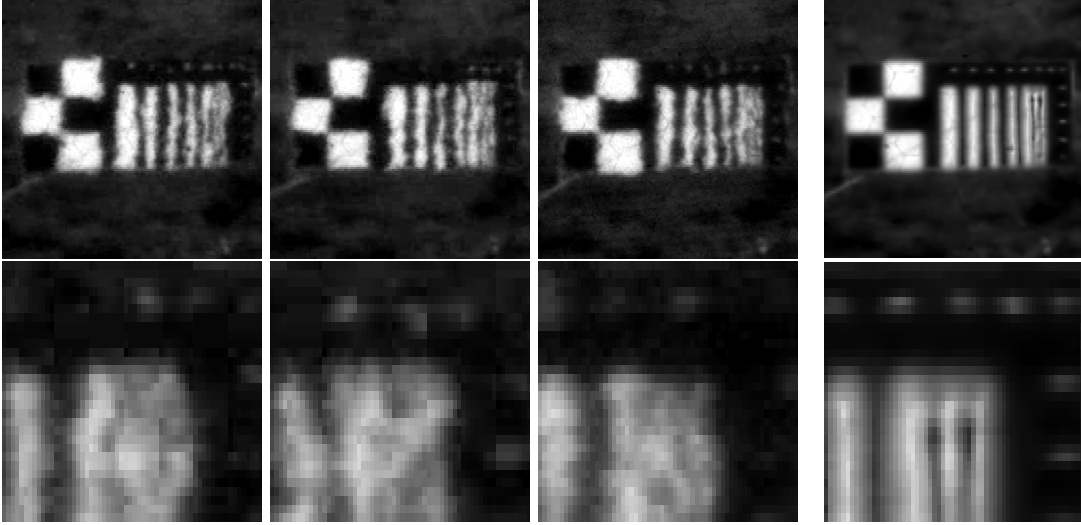


Figure 2. The first three columns are example frames and the magnification of their top right part. The last column shows our reconstructed result.

other hand, the more frames used, the longer the computational time required is. In our numerical experiments we generally observe that we can always obtain satisfactory results with only 10-30 frames. We also note that the choice of the optical flow scheme is not crucial. Experiments made via the use of the Black-Anandan algorithm, which provides a precise flow estimation but slower, or the classic Lukas-Kanade algorithm, which is faster, didn't show notable differences. As we are interested in a fast algorithm, we finally retain the Lukas-Kanade scheme in the rest of the paper. Figure 2 shows an example of the achieved result by this algorithm initially presented in.<sup>29</sup>

### 3. CHOICE OF THE REGULARIZATION

As showed in the previous section, the algorithm contains a regularization step

$$u \leftarrow \arg \min_u J(u) + \frac{\lambda}{2\delta} \|u - v\|^2 \quad (3)$$

We will now discuss the choice of  $J(u)$ . In our original work,<sup>29</sup> we choose to use the nonlocal total variation (NLTV) as the regularizing term because it was successfully used in different restoration problems and is well adapted for real images. In order to clarify our discussion, we recall the definition of NLTV.

$$J(u) = J_{NLTV}(u) = \int_{\Omega} \sqrt{\int_{\Omega} (u(y) - u(x))^2 w(x, y) dy} dx \quad (4)$$

where the weight  $w(x, y)$  corresponds to a similarity measure between patches centered on pixel  $x$  and  $y$ . As the similarity between the patches increases, so does their impact on the regularized image. It was proven that NLTV is well-adapted for images having textures or self-similarity. The main drawback of this regularizer is the time needed to compute the weight  $w(x, y)$ . In fact, the idea is to compare different patches all over the image which represents a huge number of combinations. While designing a new faster way to compute  $w(x, y)$  is completely out of the scope of this paper, we propose to study the impact of choosing other regularizers. Nowadays, some regularizers are known to be efficient and considered as "classic" in the litterature. In addition to the NLTV, we choose three other constraint terms. The probably most known in image processing is the standard total variation (TV) proposed by Rudin et al.<sup>32</sup> which preserves sharp edges in the image; it is defined by (5).

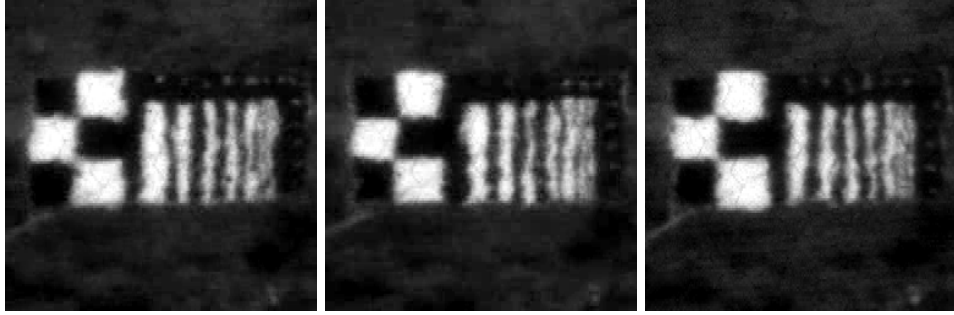


Figure 3. Input examples of the test sequence 1.

$$J(u) = J_{TV}(u) = \int_{\Omega} |\nabla u| \quad (5)$$

The other two choices are based on the idea that a regularized image will have a sparse representation in some “dictionary”. This concept is directly related to the compressive sensing theory. Here we adopt two possible tight frames as our dictionaries: framelet<sup>6,7</sup> and curvelets.<sup>8–10,14</sup> If we denote  $\mathcal{D}$  and  $\mathcal{C}$  the operators which respectively perform the framelet and curvelet expansions, the corresponding regularizers are defined by

$$J(u) = J_D(u) = \|\mathcal{D}u\|_1 \quad \text{and} \quad J(u) = J_C(u) = \|\mathcal{C}u\|_1 \quad (6)$$

Then depending on the choice of  $J(u)$ , the regularization step depicted by (3) is equivalent to

- if  $J(u) = J_{TV}(u)$ , it is the famous Rudin-Osher-Fatemi model (ROF),
- if  $J(u) = J_{NLTV}(u)$ , it is the nonlocal total variation presented at the beginning of this section,
- if  $J(u) = J_D(u)$  or  $J(u) = J_C(u)$ , it is an  $L^1 - L^2$  minimization problem widely studied in the litterature.

All of these minimization problems can be efficiently solved by the use of the Split Bregman Iterations. Corresponding Matlab routines are available in the Bregman Cookbook<sup>18</sup> or in<sup>35</sup> for NLTV.

## 4. EXPERIMENTS

We conduct our experiments on two distinct sequences (acquired during different field trials with different imaging systems), figure 3 and 4 show some randomly chosen frames from these sequences. We apply the stabilization algorithm based on the different regularizers presented in the previous section to these sequences. We keep the same set of parameters for all tests except the number  $N$  of input frames used. We perform the tests with  $N = 30$  and  $N = 100$  for sequence 1 and with  $N = 10$  and  $N = 30$  for sequence 2. Figures 5, 6, 7, 8 present outputs of the algorithm for each regularizer. Clearly, no big differences can be observed from these results, on these sequences, all regularizers perform well. Obviously TV is the fastest version of the algorithm while NLTV is the most efficient one if textures are present in the image. The approaches based on frame sparsity can provide a good tradeoff between reconstruction quality and computational speed.

## 5. CONCLUSION

In this paper we investigate the influence of the choice of the regularization term in a recent work dedicated to turbulence stabilization. We tested four of the most used regularizers in the litterature: total variation, nonlocal total variation, frame sparsity based on framelet or curvelet dictionaries. The results obtained on real images show that no major differences can be observed. The “power” of the nonlocal total variation appears in the case of textured images where it performs better but with the cost of additional computational time.

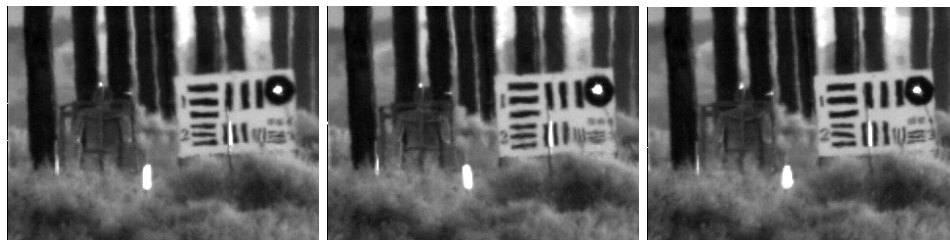


Figure 4. Input examples of the test sequence 2.

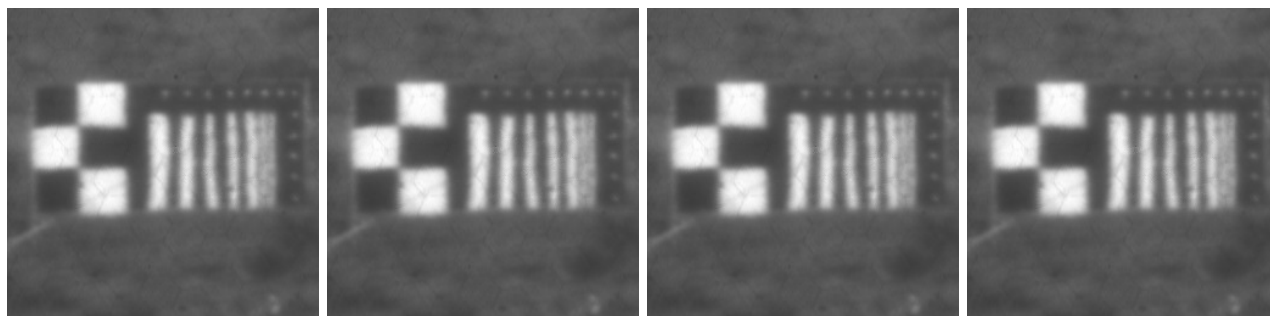


Figure 5. Restored images obtained from the different regularizers (30 input frames). From left to right: NLTV, TV, Framelet, Curvelet.

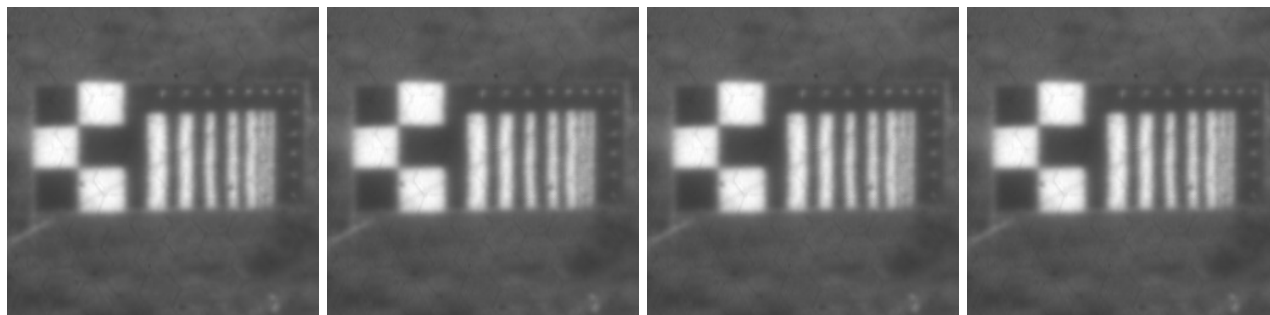


Figure 6. Restored images obtained from the different regularizers (100 input frames). From left to right: NLTV, TV, Framelet, Curvelet.



Figure 7. Restored images obtained from the different regularizers (10 input frames). From left to right: NLTV, TV, Framelet, Curvelet.

Following these results, we can suggest that, if efficiency is the major aspect which may be reached, a nonlocal total variation regularization must be preferred otherwise if the computational speed is critical, the classic total variation is the best option. If both aspects are important, then a sparsity frame based algorithm can provides the best tradeoff.



Figure 8. Restored images obtained from the different regularizers (30 input frames). From left to right: NLTV, TV, Framelet, Curvelet.

### Acknowledgment

The authors want to thank the members of the NATO SET156 (ex-SET072) Task Group for the opportunity of using the data collected by the group during the 2005 New Mexico’s field trials. This work is supported by the following grants: NSF DMS-0914856, ONR N00014-08-1-119, ONR N00014-09-1-360.

### REFERENCES

- [1] M. Almeida and L. Almeida, *Blind and Semi-Blind Deblurring of Natural Images*, IEEE Transactions on Image Processing, **19** (2010), 36–52.
- [2] M. Aubailly, M.A. Vorontsov, G.W. Carhat and M.T. Valley, *Automated video enhancement from a stream of atmospherically-distorted images: the lucky-region fusion approach*, “Proceedings of SPIE”, **7463** (2009).
- [3] M.J. Black and P. Anandan, *The robust estimation of multiple motions: Parametric and piecewise-smooth flow fields*, Comput Vision and Image Understanding, **63** (1996), 75–104.
- [4] J.Y. Bouguet, *Pyramidal Implementation of the Lucas Kanade Feature Tracker Description of the algorithm*, “Intel Corporation Microprocessor Research Labs, [http://robots.stanford.edu/cs223b04/algo\\_tracking.pdf](http://robots.stanford.edu/cs223b04/algo_tracking.pdf)” (2000).
- [5] A. Buades, B. Coll and J.M. Morel, *A review of image denoising algorithms, with a new one*, Multiscale Model Sim, **4** (2005), 490–530.
- [6] J.F. Cai, S. Osher and Z. Shen, *Linearized Bregman Iterations for Frame-Based Image Deblurring*, SIAM Journal on Imaging Sciences, **2** (2009), 226–252.
- [7] J.F. Cai, S. Osher and Z. Shen, *Split Bregman Methods and Frame Based Image Restoration*, Multiscale Modeling and Simulation, **8** (2009), 337–369.
- [8] E.J. Candès and D. Donoho, *Continuous Curvelet Transform, part I: Resolution of the Wavefront Set*, Applied Computational Harmonic Analysis Journal, **19** (2003), 162–197.
- [9] E.J. Candès and D. Donoho, *Continuous Curvelet Transform, part II: Discretization and Frames*, Applied Computational Harmonic Analysis Journal, **19** (2003), 198–222.
- [10] E. J. Candès and L. Demanet and D. L. Donoho and L. Ying, *Fast discrete curvelet transforms*, Multiscale Modeling and Simulation, **5** (2005), 861–899.
- [11] T.F. Chan and CK. Wong, *Convergence of the alternating minimization algorithm for blind deconvolution*, Linear Algebra Appl, **316** (2000), 259–285.
- [12] T.F. Chan, AM. Yip and FE. Park, *Simultaneous total variation image inpainting and blind deconvolution*, International Journal of Imaging Systems and Technology, **15** (2005), 92–102.
- [13] PL. Combettes and VR. Wajs, *Signal recovery by proximal forward-backward splitting*, Multiscale Model Sim, **4** (2005), 1168–1200.
- [14] D. Donoho and M. Duncan, *Digital curvelet transform: strategy, implementation and experiments*, Technical Report, Department of Statistics, Stanford University, 1999.
- [15] D. Frakes, J. Monaco and M. Smith, *Suppression of atmospheric turbulence in video using an adaptive control grid interpolation approach*, Proceedings of the IEEE International Conference on Acoustics, Speech, and Signal Processing (2001).

- [16] S. Gepshtein, A. Shteinman and B Fishbain, *Restoration of atmospheric turbulent video containing real motion using rank filtering and elastic image registration*, Proceedings of the Eusipco (2004).
- [17] G. Gilboa and S. Osher, *Nonlocal Operators with Applications to Image Processing*, Multiscale Model Sim, **7** (2008), 1005–1028.
- [18] J. Gilles, *The Bregman Cookbook: a Matlab toolbox implementing Bregman minimization problems*, available at <http://www.math.ucla.edu/~jegilles/BregmanCookbook.html>
- [19] J. Gilles, T. Dagobert and C De Franchis, *Atmospheric Turbulence Restoration by Diffeomorphic Image Registration and Blind Deconvolution*, in Proceedings of Advanced Concepts for Intelligent Vision Systems (ACIVS) Conference, Juan Les Pins, France (2008).
- [20] J. Gilles and S. Osher, *Fried Deconvolution*, in Proceedings of SPIE Defense, Security and Sensing conference, Baltimore, US (2012).
- [21] D. Goldfarb and W. Yin, *Parametric Maximum Flow Algorithms for Fast Total Variation Minimization*, Siam J. Sci Comput, **31** (2009), 3712–3743.
- [22] T. Goldstein and S. Osher, *The Split Bregman Method for L1 Regularized Problems*, SIAM Journal on Imaging Sciences, **2** (2009), 323–343.
- [23] L. He, A. Marquina and S. Osher, *Blind deconvolution using TV regularization and Bregman iteration*, International Journal of Imaging Systems and Technology, **15** (2005), 74–83.
- [24] M. Hirsch, S. Sra, B. Scholkopf and S. Harmeling, *Efficient filter flow for space-variant multiframe blind deconvolution*, “Computer Vision and Pattern Recognition Conference” (2010).
- [25] M. Lemaitre, “Etude de la turbulence atmosphérique en vision horizontale lointaine et restauration de séquences dégradées dans le visible et l’infrarouge”, Ph.D Thesis, Université de Bourgogne (2007).
- [26] D. Li, R.M. Mersereau and S. Simske, *Atmospheric turbulence-degraded image restoration using principal components analysis*, IEEE Geoscience and Remote Sensing Letters, **4** (2007), 340–344.
- [27] P. Lions and B. Mercier, *Splitting Algorithms for the Sum of Two Nonlinear Operators*, SIAM Journal on Numerical Analysis, **16** (1979), 964–979.
- [28] Y. Mao, B.P. Fahimian, S. Osher and J. Miao, *Development and Optimization of Regularized Tomographic Reconstruction Algorithms Utilizing Equally-Sloped Tomography*, IEEE Transactions on Image Processing, **19** (2010), 1259–1268.
- [29] Y. Mao and J. Gilles, *Non rigid geometric distortions correction - Application to atmospheric turbulence stabilization*, Accepted in the Inverse Problems and Imaging Journal (2012), Preprint available at <ftp://ftp.math.ucla.edu/pub/camreport/cam10-86.pdf>
- [30] S. Osher, M. Burger, D. Goldfarb, J. Xu and W. Yin, *An iterative regularization method for total variation-based image restoration*, Multiscale Model Sim, **4** (2005), 460–489.
- [31] GB. Passty, *Ergodic convergence to a zero of the sum of monotone operators in Hilbert space*, J. Math. Anal. Appl, **72** (1979), 383–390.
- [32] L.I. Rudin, S. Osher and E Fatemi, *Nonlinear total variation based noise removal algorithms*, Physica D: Nonlinear Phenomena, **60** (1992), 259–268.
- [33] D. Sun, S. Roth, J. Lewis and MJ. Black, *Learning optical flow*, Computer Vision–ECCV (2008).
- [34] M. Tahtali, A. Lambert and D. Fraser, *Self-tuning Kalman filter estimation of atmospheric warp*, Proceedings of SPIE (2008).
- [35] X. Zhang, M. Burger, X. Bresson and S. Osher, *Bregmanized Nonlocal Regularization for Deconvolution and Sparse Reconstruction*, SIAM Journal on Imaging Sciences, **3** (2010), 253–276. Code available at <http://www.cs.cityu.edu.hk/~xbresson/ucla/codes/NLTV.zip>
- [36] X. Zhang, M. Burger and S. Osher, *A unified primal-dual algorithm framework based on Bregman iteration*, Journal of Scientific Computing, **46** (2010), 1–27.
- [37] X. Zhu and P. Milanfar, *Image reconstruction from videos distorted by atmospheric turbulence*, “SPIE Electronic Imaging, Conference 7543 on Visual Information Processing and Communication (2010).